The American Journal of Pathology, Vol. 193, No. 2, February 2023

The American Journal of
PATHOLOGY
ajp.amjpathol.org

CARDIOVASCULAR, PULMONARY, AND RENAL PATHOLOGY

Reduction of Endothelial Glycocalyx on Peritubular Capillaries in Chronic Kidney Disease

Katja Ermert,*† Eva M. Buhl,*†‡ Barbara M. Klinkhammer,*† Jürgen Floege,† and Peter Boor*†‡

From the Institute of Pathology, the Division of Nephrology and Immunology,† and the Electron Microscopy Facility,‡ RWTH Aachen University Hospital, Aachen, Germany*

Accepted for publication November 3, 2022.

Address correspondence to Peter Boor, M.D., Ph.D., Institute of Pathology, RWTH Aachen University Hospital, Pauwelsstr. 30, 52074 Aachen, Germany.
E-mail: pboor@ukaachen.de.

In chronic kidney disease (CKD), peritubular capillaries undergo anatomic and functional alterations, such as rarefaction and increased permeability. The endothelial glycocalyx (EG) is a carbohydrate-rich gel-like mesh, which covers the luminal surface of endothelial cells. It is involved in many regulatory functions of the endothelium, including vascular permeability. Herein, we investigated ultrastructural alterations of the EG in different murine CKD models. Fluorescence staining using different lectins with high affinity to components of the renal glycocalyx revealed a reduced binding to the endothelium in CKD in the animal models, and there were similar finding in human kidney specimens. Lanthanum Dysprosium Glycosamino Glycan adhesion staining technique was used to visualize the ultrastructure of the glycocalyx in transmission electron microscopy. This also enabled quantitative analyses, showing a significant reduction of the EG thickness and density. In addition, mRNA expression of proteins involved in glycocalyx biology, synthesis, and turnover (ie, syndecan 1 and glypican 1), which are main components of the glycocalyx, and exostosin 2, involved in the synthesis of the glycocalyx, were significantly up-regulated in endothelial cells isolated from murine CKD models. Visualization of glycocalyx using specific transmission electron microscopy analyses allows qualitative and quantitative analyses and revealed significant pathologic alterations in peritubular capillaries in CKD. *(Am J Pathol 2023, 193: 138–147; https://doi.org/10.1016/j.ajpath.2022.11.003)*

Chronic kidney disease (CKD) is characterized by renal fibrosis, and peritubular capillary (PTC) rarefaction and dysfunction are proposed as important disease-driving mechanisms.[1] The endothelial glycocalyx (EG) lines the luminal surface of vascular endothelial cells, impedes platelet aggregation and inflammatory cell adhesion, and regulates vascular permeability.[2] The layer consists of proteoglycans, glycosaminoglycans, and glycoproteins.[3] During diseases, activated endothelial cells can induce the expression of heparanase and hyaluronidase, causing the degradation of the EG.[4,5] These factors are postulated to contribute to the disease pathophysiology and might lead to subsequent endothelial dysfunction.[6] Although the glycocalyx of glomerular endothelium is disrupted in disease,[7,8] there are no data available on ultrastructural alterations of EG in the PTCs in pathologic conditions. Visualization of the EG during CKD could provide a new piece of information on the spectrum of (micro)vascular damage and dysfunction in CKD and kidney fibrosis. For example, renal peritubular microvasculature becomes leaky in CKD models, but whether this could be associated with alterations of the EG is unclear.[1] Herein, the study visualized the EG in PTCs, focusing on ultrastructural morphologic assessment using the Lanthanum Dysprosium Glycosamino Glycan adhesion (LaDy GAGa).[9] A significant reduction of the EG in CKD was observed in two commonly used murine models of fibrosis and CKD with distinct disease etiology [ie, the unilateral ureteral obstruction (UUO), a model of obstructive nephropathy, and the ischemia-reperfusion (I/R) models]. Since both models are unilateral, the contralateral (unaffected) kidney can serve as an internal control.

Supported by the German Federal Ministries of Education and Research STOP-FSGS-01GM1901A (P.B.); the German Research Foundation project identifiers 322900939, 454024652, 432698239 (P.B.), and 445703531 (B.M.K. and P.B.); and the European Research Council consolidator grant AIM.imaging.CKD number 101001791 (P.B.).

K.E. and E.M.B. contributed equally to this work.

Disclosures: None declared.

https://doi.org/10.1016/j.ajpath.2022.11.003

Table 1 List of Primers Used for Quantitative Real-Time RT-PCR (All Sequences Are Given in 5′-3′ Direction)

Gene	Forward primer	Reverse primer
Mouse		
Cd31	5′-ATTGCAGTGGTTATCATCGGAGTG-3′	5′-CTCGTTGTTGGAGTTCAGAAGTGG-3′
Kdr	5′-TGGATTCCTACCAGTATGGGACC-3′	5′-TCTAGCTGCCAGTACCACTGGA-3′
Ext2	5′-GTTCCGAGGTGTGTGAGGAC-3′	5′-CGGTGCTTGGTCTTCATCCT-3′
Sdc1	5′-GAGGAGACAGAGCCTAACGC-3′	5′-GAGCGAGGGCTGTAGGTTTC-3′
Gpc1	5′-TTTGTTGTCTCCGCCTCCTC-3′	5′-GAAGGGCAGAGCCAAGGTC-3′
Gapdh	5′-GGCAAATTCAACGGCACAGT-3′	5′-AGATGGTGATGGGCTTCCC-3′

Materials and Methods

Kidney Fibrosis Animal Models

Animal experiments were performed in accordance with the guidelines for care and use of laboratory animals of the Federation of European Laboratory Animal Science Association and were approved by the local review boards (the State Office for Nature, Environment and Consumer Protection Nordrhein-Westfalen) and the animal facility of the University Clinic of the RWTH Aachen (Aachen, Germany). Mice received dry food and drinking water (ozone treated and acidified) ad libitum. Animal husbandry took place in one 12-hour light-dark cycle with a relative humidity of 45% to 65% and a room temperature of 20°C ± 2°C. Two established unilateral models of renal fibrosis with abundant capillary rarefaction were used [ie, UUO for 5 (n = 5, male) and 10 (n = 4, male) days; I/R was used for 7 (n = 2 male, 3 female) and 21 (n = 5 male) days and an additional 14 (n = 5) days for the lectin staining] in female/male 10- to 12-week−old B6 mice (Charles River, Cologne, Germany).

UUO Model

For the UUO model, mice were anesthetized by i.p. injection with ketamine/xylazine (100 + 20 mg/kg body weight), and the abdomen was opened by a median longitudinal laparotomy. The left ureter was identified and cut after ligation with 5-0 nylon suture. The two layers of the abdominal wall (muscles and skin) were closed with a 5-0 nylon seam. Analgesia was performed by s.c. administration of carprofen every 24 hours for 72 hours.

Unilateral I/R

After initiating the anesthesia with ketamine/xylazine (100 + 20 mg/kg body weight), a left-to-middle side incision was made to identify the arteries on the hilus of the left kidney and clamp them for 30 minutes. The temperature of the animal was sustained between 35°C and 37°C by a hot plate system and measured by rectal temperature. The

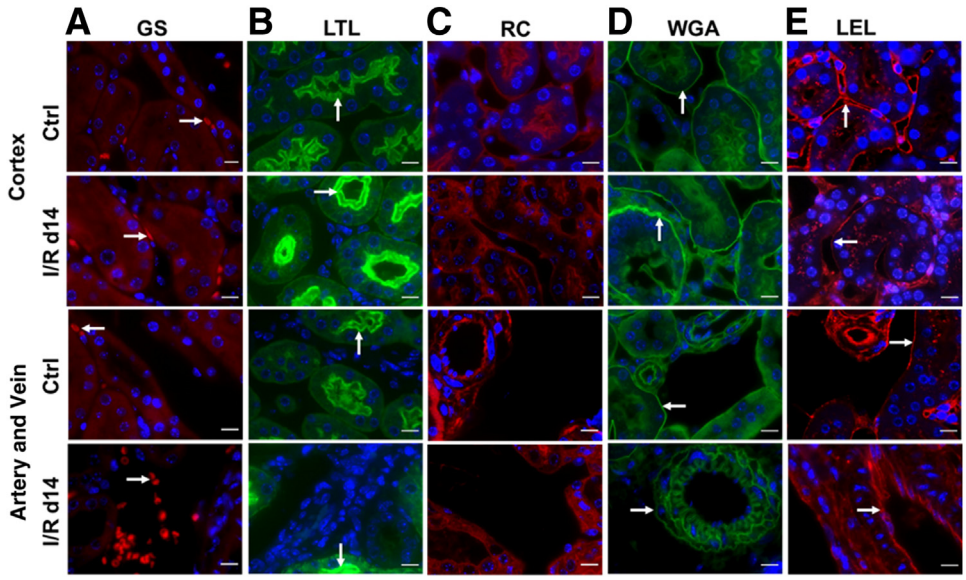

Figure 1 Fluorescence staining of various lectins to detect the alterations of the endothelial glycocalyx in renal fibrosis. **A:** *Griffonia simplicifolia* (GS) stained erythrocytes unspecifically (**arrows**). **B:** *Lotus tetragonolobus* (LTL) stains the brush border of tubular cells (**arrows**). **C:** *Ricinus communis* (RC) does not show any specific staining in the vessels. **D:** Wheat germ agglutinin (WGA) shows staining of basement membranes (**arrows**). **E:** *Lycopersicon esculentum* lectin (LEL) stains the glycocalyx of capillaries and larger vessels. In ischemia-reperfusion (I/R) injury day (d) 14, the staining of the glycocalyx is decreased in the peritubular capillaries as well as in arteries and veins (**arrow**). Nuclei were counterstained with DAPI (blue). Scale bars = 10 μm (**A**–**E**). Ctrl, contralateral kidney.

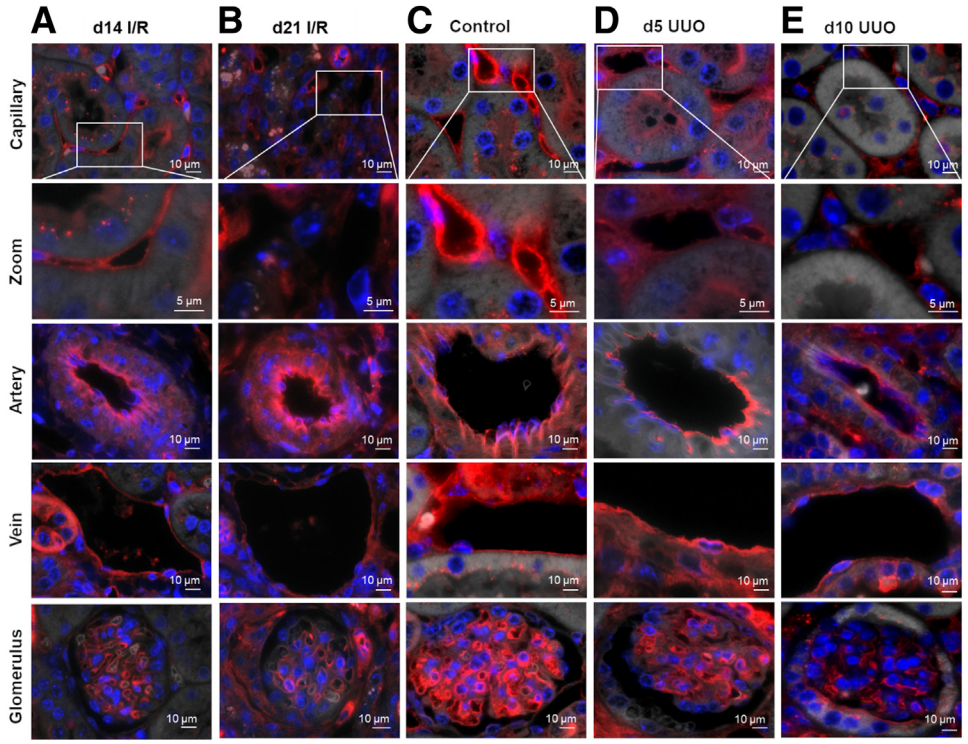

Figure 2 Decreased staining of the endothelial glycocalyx (EG) in murine renal fibrosis models using tomato *Lycopersicon esculentum* lectin (LEL). **A**–**C:** After day 14 (**A**) and 21 (**B**) of ischemia-reperfusion (I/R), the LEL binding to the EG is decreased in peritubular capillaries (PTCs) and glomerular capillaries but not markedly in larger vessels compared with the healthy murine kidney (**C**). **D** and **E:** LEL staining of the EG is reduced in kidneys after day (d) 5 and day 10 of unilateral ureteral obstruction (UUO) compared with contralateral healthy kidneys. Reduction of the staining is observed in PTCs and glomeruli, and the staining is reduced in larger vessels. Nuclei were counterstained using DAPI (blue), and tissue autofluorescence was recorded in the green fluorescent protein channel (gray). **Boxed areas:** Enlarged sections of individual capillaries (see zoom). Scale bars: 10 µm (**A**–**E**, capillary, artery, vein, and glomerulus); 5 µm (**A**–**E**, zoom).

clamp was released, and the reperfusion was verified macroscopically before two layers were sewed. Analgesia was performed by s.c. administration of carprofen every 24 hours for 72 hours.

Human Kidney Samples

Diagnostic formalin-fixed, paraffin-embedded kidney samples ($n = 3$) from the Institute of Pathology, University Hospital Aachen (Aachen, Germany), were used for fluorescence lectin staining. The study was approved by the local ethics committee (EK 042/17) and the local review boards of Aachen and was in line with the Declaration of Helsinki. Three fibrotic kidneys were used, resulting from ischemic damage after transplantation ($n = 1$) with marked fibrosis and chronic pyelonephritis with hydronephrosis, arteriolosclerosis with marked fibrosis and tubular atrophy, and global sclerosis ($n = 1$), as well as global glomerulosclerosis, interstitial fibrosis, and tubular atrophy ($n = 1$). In all cases, the vasculature was affected, leading to reduced PTC. Nonfibrotic/healthy kidney tissue was obtained from nephrectomy specimen of discarded transplant kidney ($n = 1$; ischemic time about 25 hours at 4°C). All human tissues were immersion fixed.

Fluorescence Staining

Formalin-fixed, paraffin-embedded tissue slides were divided into sections (1 µm thick). The deparaffinized and rehydrated slides were incubated with fluorescently labeled lectins from *Griffonia simplicifolia* (+fluorescein isothiocyanate) (Vector Laboratories, Burlingame CA), *Lotus tetragonolobus* (+fluorescein), *Ricinus communis* (+fluorescein) (Vector Laboratories), wheat germ agglutinin (+fluorescein) (Vector Laboratories), and *Lycopersicon esculentum* lectin (LEL; +Dylight488) (Vector Laboratories). The cell nuclei were counterstained with DAPI (Roche, Mannheim, Germany) for 10 minutes, washed three times in Aqua dest. (in-house preparation), and covered with Immu-Mount (Thermo Fisher Scientific, Reinach, Switzerland). All samples were imaged using a digital widefield fluorescence microscope (Axio Imager 2; Zeiss, Oberkochen, Germany), and all micrographs were acquired with the same exposure time.

Isolation of Primary Peritubular Endothelial Cells from Murine Tissue

For the examination of the alterations of EG in fibrosis, primary endothelial cells from PTCs were isolated from murine kidneys. The donor animal was perfused with saline

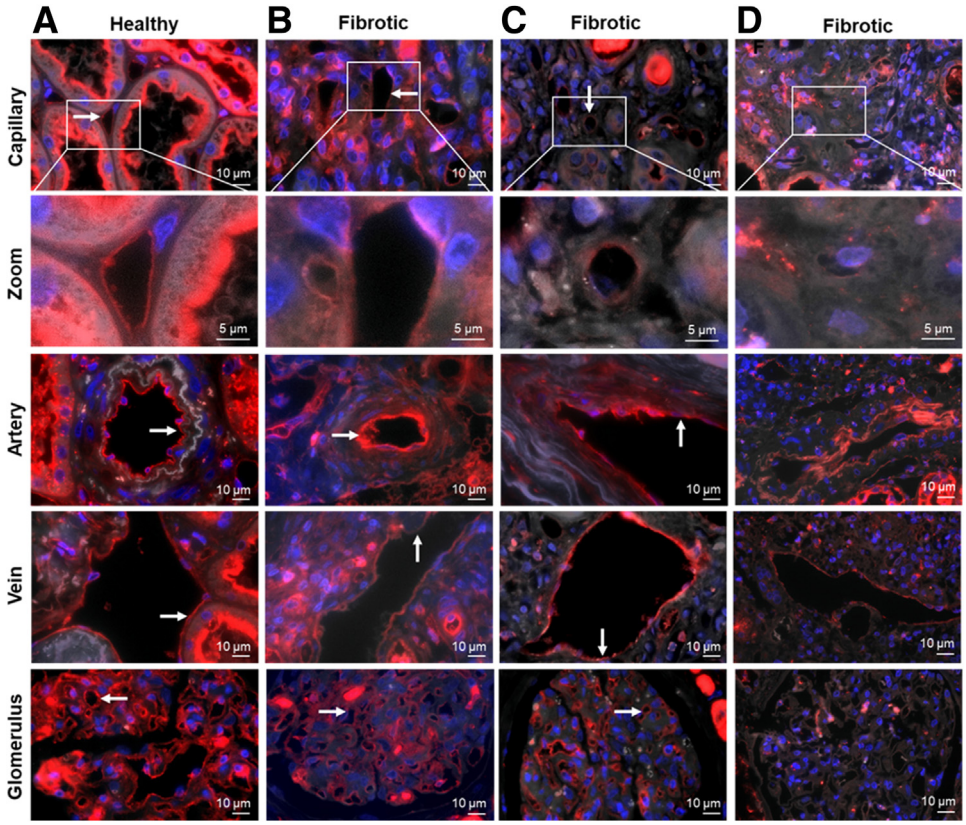

Figure 3 Decrease tomato lectin [*Lycopersicon esculentum lectin* (LEL)] signal in human renal fibrosis. **A:** Fluorescence images showing LEL stains endothelial glycocalyx (EG) in arteries, veins, and capillaries of peritubular capillaries (PTCs) and glomeruli of healthy human kidney (**arrows**). **B:** A kidney biopsy from a transplanted kidney after cold ischemia (30 minutes) stained with LEL shows less staining of the EG in veins and capillaries of PTCs and glomeruli (**arrows**). **C:** LEL staining is reduced in biopsy of chronic diseased human kidney (chronic pyelonephritis with hydronephrosis, arteriolosclerosis with marked fibrosis, tubular atrophy, and global sclerosis; **arrows**). **D:** LEL staining is reduced in biopsy of chronic diseased human kidney (global sclerosis with marked fibrosis and tubular atrophy). Reduction of the staining is observed in kidney capillaries of PTCs and glomeruli, but not markedly in arteries and veins (**arrow**). Nuclei were counterstained with DAPI (blue). **Boxed areas:** Enlarged sections of individual capillaries (see zoom). Scale bars: 10 µm (**A**—**D**, capillary, artery, vein, and glomerulus); 5 µm (**A**—**D**, zoom).

through the left ventricle of the heart. The kidney cortex was dissected from the medulla, and the tissue was dissociated using gentleMACS Dissociator with the Multi Tissue Dissociation Kit 1 (Miltenyi Biotec, Bergisch Gladbach, Germany) at 37°C. The suspension was sieved with a 40-µm pore size cell strainer to sort out bigger structures, particularly glomeruli and bigger vessels. The single-cell suspension was incubated and stained with antibodies against the endothelial markers CD31 (BioLegend, San Diego, CA), CD45 (Invitrogen, Carlsbad, CA), as well as DAPI. Fluorescence-activated cell sorting was used for the separation of primary endothelial cells and was courtesy and performed by Carmen Tag and Ralf Weißkirchen (University Clinic of the RWTH Aachen). Primary endothelial cells ($CD31^+$, $CD45^-$, and $DAPI^-$) were separated from dead cells ($DAPI^+$) and immune cells ($CD45^+$).

Quantitative Real-Time RT-PCR

cDNA synthesis and the quantitative real-time RT-PCR was performed as described previously.[10–12]

The quantitative real-time RT-PCR was performed with the ABI Prism 7300 sequence detection system (Applied Biosystems, Weiterstadt, Germany). Each reaction contained 0.75 µL of cDNA and was amplified in a 25-µL volume using the qPCR Core Kit for SYBR Green I (Eurogentec, Seraing, Belgium). Each sample was assayed in duplicates. The PCR conditions consisted of 50°C for 2 minutes, followed by 40 cycles of 95°C for 15 seconds and 60°C for 1 minute. Primers were designed from sequences in the GenBank database using National Center for Biotechnology Information's PRIMER BLAST. Primer sequences are listed in Table 1. Glyceraldehyde-3-phosphate dehydrogenase was used as an internal standard in all measurements. The analysis was performed using the C_T value (cycle threshold) method.

Glycocalyx Probes and Staining with LaDy GAGa

UUO (5 and 10 days) and I/R injury (7 and 21 days) were used as murine renal fibrosis models. At the time of sacrifice, anesthetized mice were perfused by injection with

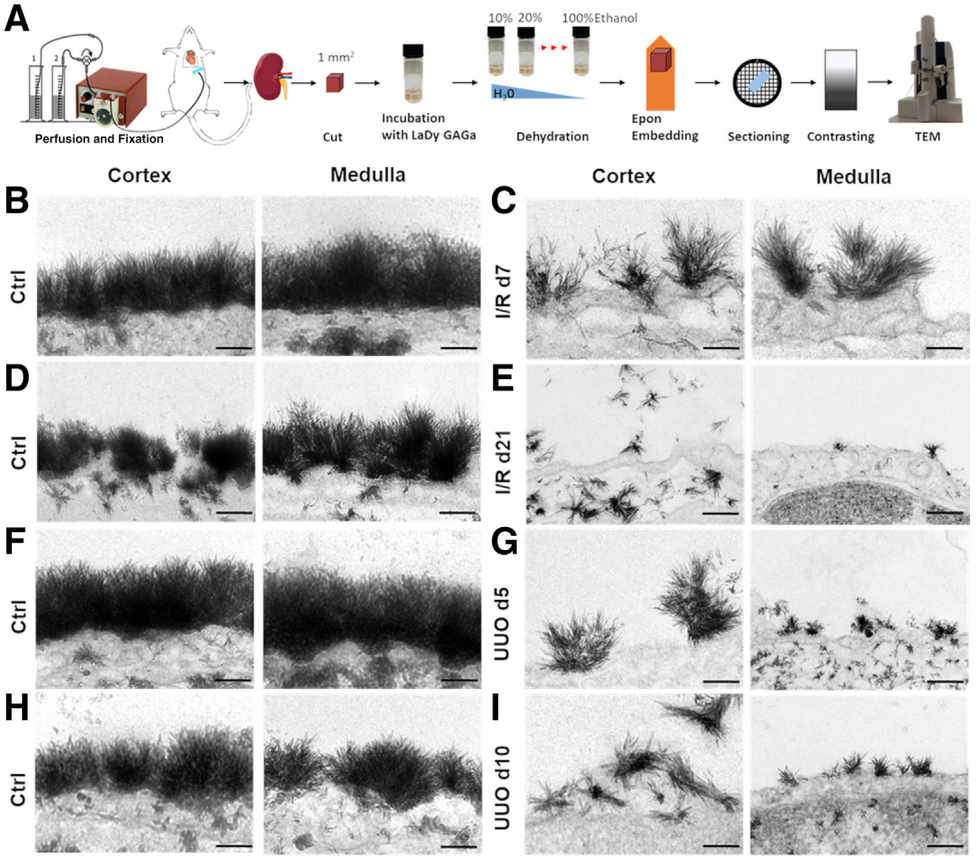

Figure 4 Ultrastructural changes of the renal endothelial glycocalyx (EG) using transmission electron microscopy (TEM). **A:** Glycocalyx sample preparation and Lanthanum Dysprosium Glycosamino Glycan adhesion (LaDy GAGa) staining technique. **B**, **D**, **F**, and **H:** Representative electron micrographs of capillaries of the cortex and medulla of contralateral kidneys (Ctrl) show a densely packed EG, similar in length and density. **C**, **E**, **G**, and **I:** Endothelium of capillaries shows ultrastructural alterations of the glycocalyx, in two fibrosis models and two time points each [unilateral ureteral obstruction (UUO) day (d) 5 and 10, ischemia-reperfusion (I/R) day 7 and 21] of murine kidneys stained with LaDy GAGa. The EG of fibrotic kidneys is markedly reduced in thickness and density compared with contralateral kidneys. Scale bars = 100 nm (**B**–**I**).

physiological saline into the left ventricle of the heart with an opened vena cava to remove all blood.

Preservation of the tissue and glycocalyx was ensured by the perfusion with fixing solution (2.5% glutaraldehyde in 0.1 mol/L Sørensen-phosphate buffer). Kidney tissue was cut into 1-mm^3 small pieces and placed in fixing solution for 2 to 4 hours.

For the glycocalyx visualization, the samples were stained with 1% LaDy GAGa solution [1% Lanthanum (III) nitrate hexahydrate (Merck, Darmstadt, Germany) and 1% Dysprosium (III) chloride hexahydrate (Merck) in NaCl and 1% HEPES] for 1 hour. Samples were further processed for electron microscopy. The glycocalyx was examined using a Hitachi HT7800 transmission electron microscope (Hitachi, Tokyo, Japan) operating at an acceleration voltage of 100 kV.

Transmission Electron Microscopy

After LaDy GAGa staining tissue samples were post-fixed in 1% OsO_4 (Science Services, Munich, Germany) in 25 mmol/L sucrose buffer and dehydrated by an ascending percentage of an alcohol row (30, 50, 70, 90, and 3 × 100%). Subsequently, the samples were incubated first in propylene oxide (Serva, Heidelberg, Germany), in a mixture of Epon resin (Serva) and propylene oxide (1:1) and finally in pure Epon. Samples were embedded in pure Epon and polymerized at 90°C for 2 hours.

Ultrathin sections (90 to 100 nm) were cut by an ultramicrotome (Ultracut UC6; Leica, Wetzlar, Germany) with a diamond knife (Diatome, Nidau, Switzerland) and picked up on Cu/Rh grids (HR23 Maxtaform; Plano, Wetzlar, Germany).

The contrast was enhanced by staining with 0.5% uranyl acetate and 1% lead citrate (both from EMS, Munich, Germany). The glycocalyx was examined using a Hitachi HT7800 transmission electron microscope operating at an acceleration voltage of 100 kV. The thickness of the glycocalyx was measured at three randomly selected points in 15 images of each sample using ImageJ software version 1.45s (NIH, Bethesda, MD; *https://imagej.nih.gov/ij/download.html*, last accessed May 24, 2021). The density

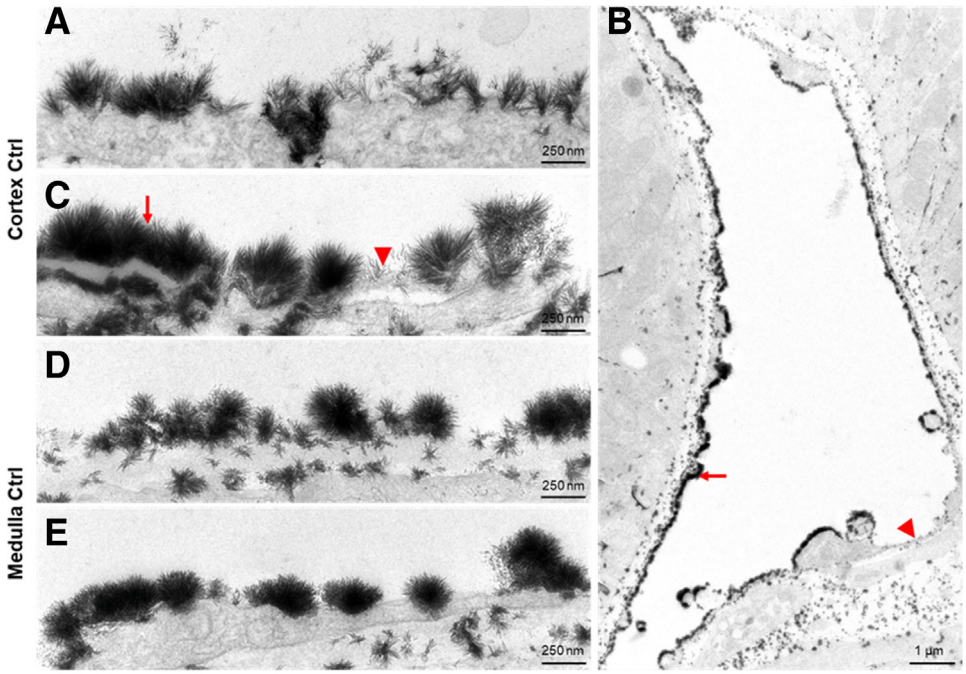

Figure 5 Variability of the visualized glycocalyx within one capillary in transmission electron microscopy. Within the sample series, the staining of the glycocalyx of contralateral kidneys (Ctrl) with Lanthanum Dysprosium Glycosamino Glycan adhesion method shows a high variability. **A** and **C:** The variance of the stained glycocalyx in the cortex of contralateral kidneys with glycocalyx either stains dense (**arrow**) or reduces in length and density (**arrowhead**). **B:** This variance, from a densely stained glycocalyx (**arrowhead**) on one that appeared to be reduced in length and density (**arrow**), was considered for the quantification. **D** and **E:** Two samples of the medulla of healthy mice also show variance in staining. Scale bars: 250 nm (**A** and **C**–**E**); 1 µm (**B**).

was determined over the entire length of the glycocalyx on 15 randomly chosen images (=15 capillaries) per sample by measuring the stained area in percentage of a capillary per image. The average thickness and density were calculated per animal. All analyses were performed in a blinded manner.

Statistical Analysis

All data are presented as individual values and means ± SD. GraphPad Prism version 6.01 (GraphPad Software Inc., San Diego, CA) was used for statistical analysis. Paired *t*-tests were used to compare data from fibrotic and contralateral kidneys from the same animals. One-way analysis of variance, followed by Bonferroni correction, was used for comparing more than two groups. Statistical significance was defined as $P < 0.05$.

Results

Decreased LEL Staining Depicts the Loss of EG in Murine Fibrosis Models

In murine kidney sections stained with plant-derived lectins (Figure 1), LEL marked all types of vessels (ie, PTCs, arteries, and veins) (Figure 1), whereas the other four tested lectins did not specifically stain the vasculature. Fluorescence images showed a reduced LEL staining in kidneys after 5 and 10 days of UUO and after 14 and 21 days of I/R-induced fibrosis compared with contralateral healthy kidneys (Figure 2). The reduction was predominantly observed in peritubular and glomerular capillaries and to a lower extent also in arteries and veins (Figure 2).

Similar findings of reduced LEL staining were observed in human kidney biopsies with fibrosis. In these kidneys, the capillaries in the interstitium and glomeruli showed less LEL staining compared with a healthy human kidney section (Figure 3). The LEL staining in large arteries and veins was not markedly reduced.

Ultrastructural Alterations of the Glycocalyx

To analyze ultrastructural alterations of the EG, a transmission electron microscopy (TEM) method was tested and adapted, allowing the visualization and quantification of the thickness and density of the EG in PTCs (Figure 4A). For the visualization of the EG, various techniques were tested to overcome the problem of low contrast of EG.

Ruthenium red, with a better affinity for chondroitin and heparan sulfate, or perfusion through the heart, was tested, but without success.[13] In contrast, reproducible staining of EG could be achieved with the use of lanthanum and dysprosium ions. Healthy kidneys showed a dense layer of the EG at the apical luminal side of the endothelium and within the

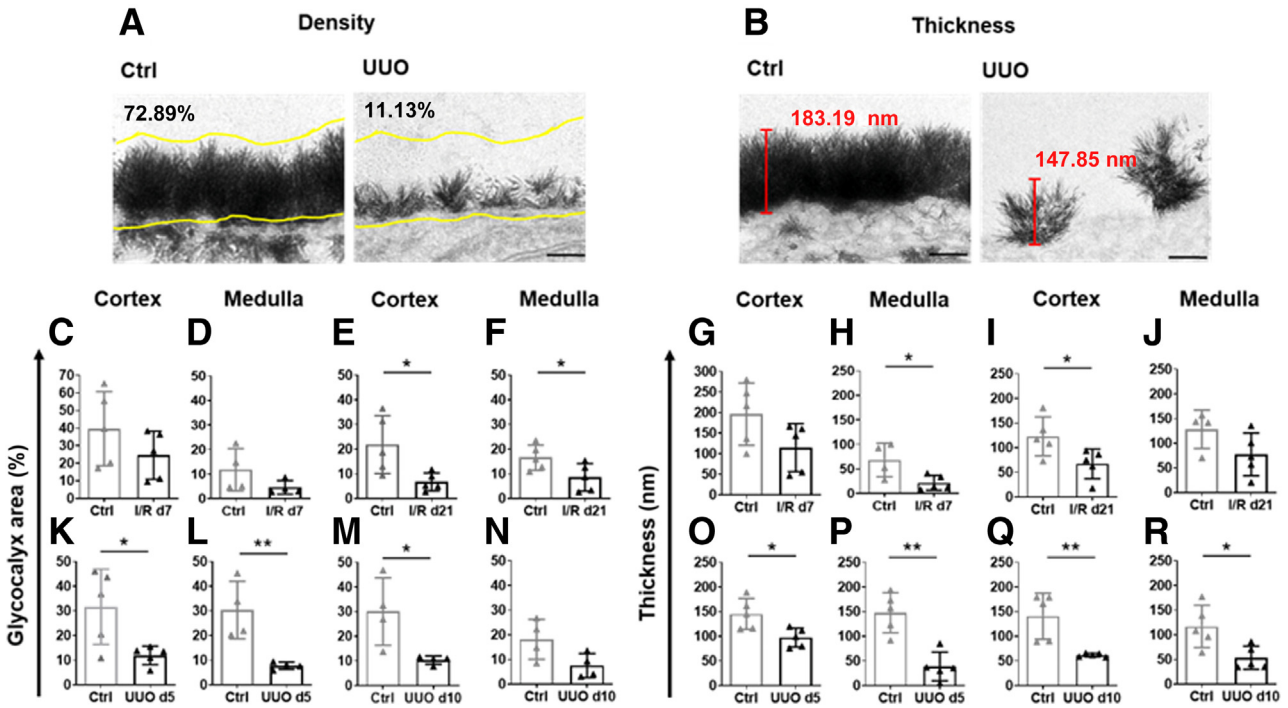

Figure 6 Quantification of the ultrastructural alterations of the density and thickness of glycocalyx. **A**, **C**—**F**, and **K**—**N:** Measurement of density and thickness of the glycocalyx with ImageJ software after staining with Lanthanum Dysprosium Glycosamino Glycan adhesion (**yellow lines**: examples of measurement of glycocalyx layer density by measuring the percentage of stained area between the two lines. **B**, **G**—**J**, and **O**—**R:** The density of the endothelial glycocalyx (EG) is reduced in two fibrosis models [day (d) 5 and 10 unilateral ureteral obstruction (UUO), day 7 and 21 ischemia-reperfusion (I/R)] of murine kidneys compared with contralateral healthy kidneys (Ctrl). Reduction of the density is observed in the kidney cortex and medulla. Under healthy conditions, the thickness varies between 100 and 200 nm. (**Red bars**: examples of measurements of the thickness of the glycocalyx.) **G** and **J:** The thickness of the EG is reduced in the cortex of I/R day 7 and the medulla of day 21 I/R. **H** and **I:** In the medulla of day 7 I/R and the cortex of day 21 I/R, the thickness is significantly reduced. The thickness of the EG is significantly reduced in both time points of the fibrosis model (day 5 and10 UUO) of murine kidneys compared with contralateral healthy kidneys. $n = 4$ to 5 (**C**—**R**). $^{*}P < 0.05$, $^{**}P < 0.01$ versus contralateral kidney (*t*-test). Scale bars = 100 nm (**A** and **B**).

endothelial fenestrations (Figure 4, B, D, F, and H). In both I/R and UUO, at early time points (day 7 I/R and day 5 UUO), the EG showed a patchy loss, shedding from the endothelium surface, and reduced density (Figure 4, C and G).

A further reduction of the glycocalyx (Figure 4, E and I) was observed with the progression of disease and fibrosis. Similar changes were observed in the kidney cortex and medulla. The thickness of the glycocalyx was 100 to 200 nm in contralateral (unaffected) kidneys, and 50 to 100 nm in fibrotic kidneys.

The staining showed variability among individual PTCs (Figure 5). Within one capillary cross-section, there was continuously stained EG, but some PTCs showed reduced density and thickness of the EG. This variance was considered in the quantification by including 15 PTCs per sample in the analyses. Quantification of the ultrastructural EG alterations confirmed the reduction of the density (Figure 6, A, C—F, and K—N) and thickness (Figure 6, B, G—J, and O—R) in both the cortex and medulla of murine fibrotic kidneys compared with the contralateral kidneys. Although no indication of sex-specific effects was found on glycocalyx, this study was not designed to assess such changes.

Increased Expression of the Glycocalyx Components in CKD Models

Expression of two glycocalyx components, glypican-1 (*Gpc1*) and syndecan-1 (*Sdc1*), and the enzyme exostosin-2 (*Ext2*) involved in the synthesis of the glycocalyx, was measured. The mRNA expression was analyzed specifically in primary murine endothelial cells isolated from the cortex of healthy and diseased I/R and UUO kidneys (Figure 7). Exostosin-2 and syndecan-1 were significantly, and glypican-1 was not significantly, increased in endothelial cells from mice with fibrosis, independently of the model (Figure 7).

Discussion

This study analyzed the EG in murine kidneys by microscopic and ultrastructural visualization to gain a better understanding of the changes during fibrosis and CKD.

LEL staining revealed a decreased staining of the EG in PTCs, glomerular, and larger vessels of murine renal fibrosis models. Lectins bind to specific sugar moieties of

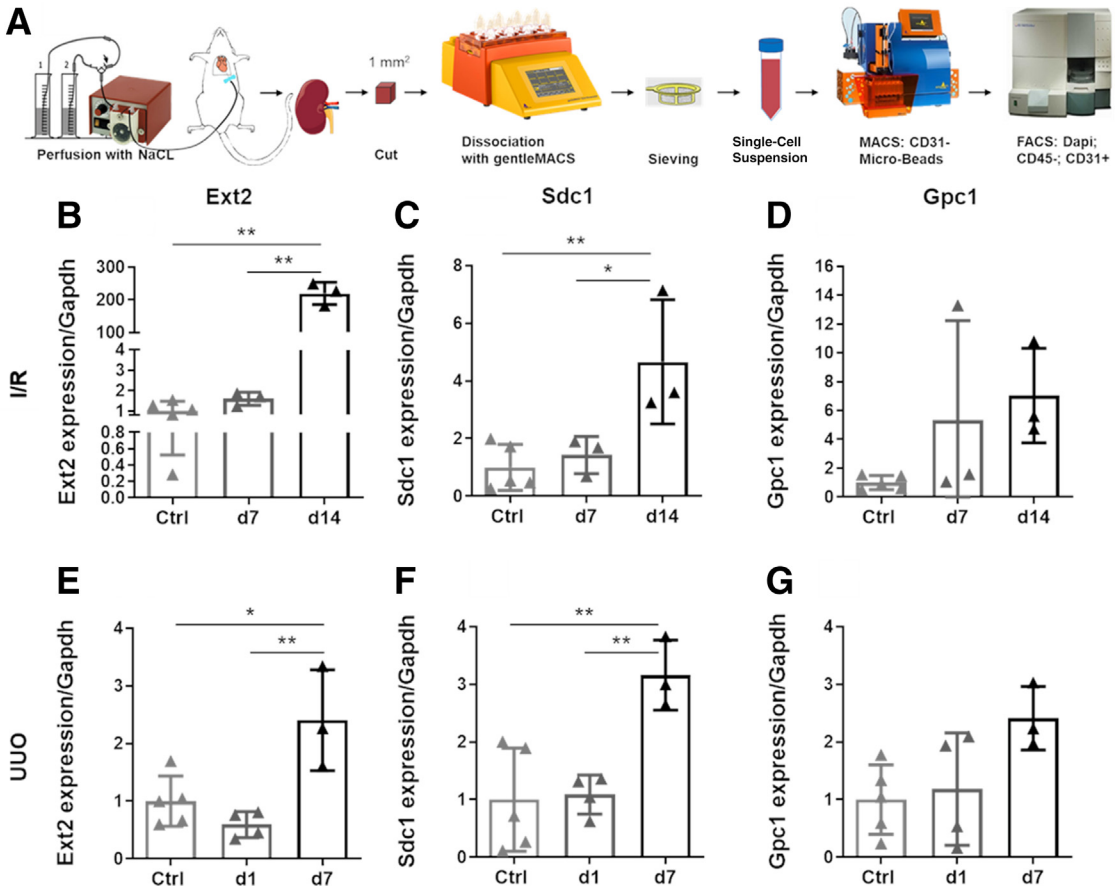

Figure 7 Loss of the glycocalyx leads to an increase of the glycocalyx component expression. **A:** Isolation of primary peritubular endothelial cells from murine tissue. **B**–**G:** Expression levels of the two components glypican-1 (Gpc1) and syndecan-1 (Sdc1) and the enzyme exostosin-2 (Ext2) involved in glycocalyx synthesis, measured in primary peritubular endothelial cells in two murine fibrosis models [day (d) 1 and 7 unilateral ureteral obstruction (UUO), day 7 and 14 ischemia-reperfusion (I/R)]. **B**, **C**, **E**, and **F:** The mean expression of Ext2 and Sdc1 significantly increased fibrosis induced by UUO and I/R. **D** and **G:** The average of Gpc1 was increased in the kidneys of both fibrosis models. $n = 3$ to 5 (**B-G**). $^{*}P < 0.05$, $^{**}P < 0.01$ (analysis of variance, post hoc Tukey test). Ctrl, contralateral kidney.

glycosaminoglycan chains of the EG, which are involved in important functions for the endothelium, including interactions with plasma proteins and leukocytes.[14] This renders lectins an effective staining and simple tool for imaging the EG morphology and studying its alterations in CKD. Staining of the glycocalyx in histologic sections allowed simple morphologic examination of the microvasculature under the fluorescence microscope. The properties of LEL binding conserved in paraffin-embedded kidney tissue allowed analysis of archival samples. Lectins can be fluorescently or biotin labeled, enabling a variety of other imaging techniques. This method was used to show a reduction in the glycocalyx of PTCs in diseased conditions.

Measuring the size and density of the glycocalyx is only possible via electron microscopy. However, it is a challenging task, because visualization via TEM needs heavy metal staining. Also, preservation by an appropriate fixation technique is crucial to ensure that the glycocalyx does not tear off or shrink during the preparation. Proper staining could not be achieved without perfusion fixation, making this method unusable for human biopsy material.

Several different methods have been used in the past for TEM analyses. The first TEM images of the glycocalyx were obtained in 1966 via staining with Ruthenium Red in combination with glutaraldehyde/osmium tetroxide fixation. The average thickness of the capillary glycocalyx was reported to be around 20 nm. Since then, the method has been continuously improved with regard to the dye, fixation, and prevention of dehydration.[15] For example, Ruthenium Red staining was limited by its relatively large molecular size, which prevented access to the whole glycocalyx layer. Moreover, it may change the glycocalyx geometry by electrostatic effects. To overcome these limitations, a smaller molecule was used. The dye Alcian blue forms an osmiophilic complex with glutaraldehyde and provides additional information about the charge density and the nature of the anionic groups in the colored regions.[16] In rat myocardial vessels, a 200 to 500 nm thick glycocalyx

covering the endothelium has been described using Alcian blue.[17] However, washing steps required with this technique probably remove plasma proteins at membrane-bound glycoproteins of the glycocalyx.[16] In the novel LaDy-GAGa method, developed by Arkill et al,[3,9] the glycocalyx is fixed not only by buffered glutaraldehyde solution, but also by diffusion with the trivalent lanthanide and dysprosium ions that bind to glycosaminoglycans. The dysprosium ions are smaller and penetrate into smaller spaces, but react with glycocalyx in a similar manner.[3] With this method, a thickness of the glycocalyx in TEM of 60 to 100 nm was measured in glomerular capillaries.[18] It currently remains unclear whether glycocalyx thickness might differ between various (micro)vascular beds of different organs and tissues, which might also explain different results of the studies.

The LaDy GAGa staining technique was chosen for current analyses because it was the most reproducible and robust staining compared with Alcian blue or Ruthenium Red staining (data not shown).[19] Herein, the published protocol was changed slightly to better implement it into the current workflow (ie, perfusion fixation before staining, followed by immersion staining with LaDy GAGa staining solution). This method reduced the risk of shedding the glycocalyx by shear stress due to shorter perfusion times.

The average thickness of the PTC glycocalyx was found to be 100 to 200 nm in unaffected kidneys and 50 to 100 nm in fibrotic kidneys. However, in diseased kidneys, that capillaries may be partially retarded and clogged with microthrombi, hindering proper perfusion. In nonperfused capillaries, the glycocalyx staining was not successful. Therefore, only capillaries free of blood residues were chosen for the current analyses. Unaffected kidneys were used as control. Although these are healthy in principle, they are subjected to increased perfusion pressure to compensate for the failure of the injured kidney. The possibility that that this might potentially affect the glycocalyx cannot be excluded.

Herein, this method was used to find a loss of the EG from the endothelial surface with a reduction in density and thickness in two different fibrosis models. Data showing altered glycocalyx in peritubular capillaries in CKD might spark further research on the pathophysiological role of glycocalyx in progression of kidney diseases. The EG quantification could be used as a readout for experimental studies analyzing the pathophysiological role of kidney microvasculature. For example, reduced EG increased the risk for organ injury in diabetes, sepsis, and atherosclerosis, probably due to increased permeability.[8] Experimental EG removal analyzed in glomeruli was directly associated with albuminuria and proteinuria.[20]

The EG constituents vary according to tissue and cell type but are primarily composed of glycosaminoglycans and proteoglycans, belonging to the main families of syndecans and glypicans.[21] Glycocalyx components are expressed on every cell in the human body.[22] Therefore, to specifically analyze the expression of EG components required the isolation of endothelial cells from peritubular capillaries. The current study demonstrated increased syndecan-1 and glypican-1 expression as a result of vascular injury in the latter stages of the two murine models of fibrosis, confirmed by the results of publicly available RNA-sequencing data. Elevated plasma concentrations of syndecan-1 are associated with trauma and sepsis to indicate acute glycocalyx degradation.[23] An increase in glypican-1 and exostosin-2 has also been reported in experiments on isolated beating guinea pig hearts, in a melanoma mouse model, and in patients with sepsis.[24,25]

Taken together, the study quantified alterations of kidney endothelial glycocalyx of peritubular capillaries, focusing on ultrastructural assessment using the LaDy GAGa method, which revealed glycocalyx loss in experimental kidney fibrosis and CKD. These methods and findings might help to analyze changes in the microvasculature and the association of EG alterations in progressive kidney disease, providing new insights into microvascular dysfunction in CKD.

Acknowledgments

We thank Jana Baues, Louisa Böttcher, Christina Gianussis, Simon Otten, and Marie Cherelle Timm for technical assistance in histopathology. Image templates provided by Servier Medical Art were employed for preparing the graphical abstract.

References

1. Bábíčková J, Klinkhammer BM, Buhl EM, Djudjaj S, Hoss M, Heymann F, Tacke F, Floege J, Becker JU, Boor P: Regardless of etiology, progressive renal disease causes ultrastructural and functional alterations of peritubular capillaries. Kidney Int 2017, 91:70−85
2. Menshikh A, Scarfe L, Delgado R, Finney C, Zhu Y, Yang H, de Caestecker MP: Capillary rarefaction is more closely associated with CKD progression after cisplatin, rhabdomyolysis, and ischemia-reperfusion-induced AKI than renal fibrosis. Am J Physiol Renal Physiol 2019, 317:F1383−F1397
3. Arkill KP, Neal CR, Mantell JM, Michel CC, Qvortrup K, Rostgaard J, Bates DO, Knupp C, Squire JM: 3D reconstruction of the glycocalyx structure in mammalian capillaries using electron tomography. Microcirculation 2012, 19:343−351
4. Rehm M, Bruegger D, Christ F, Conzen P, Thiel M, Jacob M, Chappell D, Stoeckelhuber M, Welsch U, Reichart B, Peter K, Becker BF: Shedding of the endothelial glycocalyx in patients undergoing major vascular surgery with global and regional ischemia. Circulation 2007, 116:1896−1906
5. Rahbar E, Cardenas JC, Baimukanova G, Usadi B, Bruhn R, Pati S, Ostrowski SR, Johansson PI, Holcomb JB, Wade CE: Endothelial glycocalyx shedding and vascular permeability in severely injured trauma patients. J Transl Med 2015, 13:117
6. Liew H, Roberts MA, Macginley R, McMahon LP: Endothelial glycocalyx in health and kidney disease: rising star or false dawn? Nephrology 2017, 22:940−946
7. Singh A, Satchell SC, Neal CR, McKenzie EA, Tooke JE, Mathieson PW: Glomerular endothelial glycocalyx constitutes a barrier to protein permeability. J Am Soc Nephrol 2007, 18:2885

8. Butler MJ, Down CJ, Foster RR, Satchell SC: The pathological relevance of increased endothelial glycocalyx permeability. Am J Pathol 2020, 190:742−751
9. Arkill KP, Qvortrup K, Starborg T, Mantell JM, Knupp C, Michel CC, Harper SJ, Salmon AH, Squire JM, Bates DO, Neal CR: Resolution of the three dimensional structure of components of the glomerular filtration barrier. BMC Nephrol 2014, 15:24
10. Klinkhammer BM, Kramann R, Mallau M, Makowska A, van Roeyen CR, Rong S, Buecher EB, Boor P, Kovacova K, Zok S, Denecke B, Stuettgen E, Otten S, Floege J, Kunter U: Mesenchymal stem cells from rats with chronic kidney disease exhibit premature senescence and loss of regenerative potential. PLoS One 2014, 9: e92115
11. Djudjaj S, Lue H, Rong S, Papasotiriou M, Klinkhammer BM, Zok S, Klaener O, Braun GS, Lindenmeyer MT, Cohen CD, Bucala R, Tittel AP, Kurts C, Moeller MJ, Floege J, Ostendorf T, Bernhagen J, Boor P: Macrophage migration inhibitory factor mediates proliferative GN via CD74. J Am Soc Nephrol 2016, 27: 1650−1664
12. Buhl EM, Djudjaj S, Babickova J, Klinkhammer BM, Folestad E, Borkham-Kamphorst E, Weiskirchen R, Hudkins K, Alpers CE, Eriksson U, Floege J, Boor P: The role of PDGF-D in healthy and fibrotic kidneys. Kidney Int 2016, 89:848−861
13. Chevalier L, Selim J, Genty D, Baste JM, Piton N, Boukhalfa I, Hamzaoui M, Pareige P, Richard V: Electron microscopy approach for the visualization of the epithelial and endothelial glycocalyx. Morphologie 2017, 101:55−63
14. Singh A, Fridén V, Dasgupta I, Foster RR, Welsh GI, Tooke JE, Haraldsson B, Mathieson PW, Satchell SC: High glucose causes dysfunction of the human glomerular endothelial glycocalyx. Am J Physiol Renal Physiol 2011, 300:F40−F48
15. Luft JH: Fine structures of capillary and endocapillary layer as revealed by ruthenium red. Fed Proc 1966, 25:1773−1783
16. Pries AR, Secomb TW, Gaehtgens P: The endothelial surface layer. Pflugers Arch 2000, 440:653−666
17. Van Den Berg BM, Vink H, Spaan JAE: The endothelial glycocalyx protects against myocardial edema. Circ Res 2003, 92:592−594
18. Rostgaard J, Qvortrup K: Electron microscopic demonstrations of filamentous molecular sieve plugs in capillary fenestrae. Microvasc Res 1997, 53:1−13
19. Arkill KP, Knupp C, Michel CC, Neal CR, Qvortrup K, Rostgaard J, Squire JM: Similar endothelial glycocalyx structures in microvessels from a range of mammalian tissues: evidence for a common filtering mechanism? Biophys J 2011, 101:1046−1056
20. Salmon AHJ, Ferguson JK, Burford JL, Gevorgyan H, Nakano D, Harper SJ, Bates DO, Peti-Peterdi J: Loss of the endothelial glycocalyx links albuminuria and vascular dysfunction. J Am Soc Nephrol 2012, 23:1339−1350
21. Hahn RG, Zdolsek M, Zdolsek J: Plasma concentrations of syndecan-1 are dependent on kidney function. Acta Anaesthesiol Scand 2021, 65: 809−815
22. Möckl L: The emerging role of the mammalian glycocalyx in functional membrane organization and immune system regulation. Front Cell Dev Biol 2020, 8:253
23. Fisher J, Linder A, Bentzer P: Elevated plasma glypicans are associated with organ failure in patients with infection. Intensive Care Med Exp 2019, 7:2
24. Melrose J: Glycosaminoglycans in wound healing. Bone Tissue Regen Insights 2016, 7. BTRI.S38670
25. Lipowsky HH: Protease activity and the role of the endothelial glycocalyx in inflammation. Drug Discov Today Dis Models 2011, 8: 57−62